Contract Imaging Services at the Nikon BioImaging Lab

Nikon BioImaging Lab is a state-of-the-art facility located in Cambridge, Massachusetts, that provides advanced technologies to support the burgeoning regenerative medicine and biotech sector. At the lab, Nikon offers the expertise and equipment required to carry out simple to complex cell-based imaging assays. The facility is equipped to handle the complete assay process, cell thawing, expansion, differentiation, drug and toxicology screening, image data acquisition, and image data analysis.

For more information on Nikon's contract imaging services, visit www.microscope.healthcare.nikon.com/bioimaging-lab

nikon-instruments-inc- nikoninstrumentsinc nikoninst nikoninstruments
Nikon Instruments Inc. | www.microscope.healthcare.nikon.com | nikoninstruments@nikon.net

STEM CELLS®

CANCER STEM CELLS

A Novel Oncogenic Role of Inositol Phosphatase SHIP2 in ER-Negative Breast Cancer Stem Cells: Involvement of JNK/Vimentin Activation

CHIUNG-HUI FU,[a,b,c] RUEY-JEN LIN,[b,c] JOHN YU,[c,d] WEN-WEI CHANG,[b,e,f] GUO-SHIOU LIAO,[g] WEN-YING CHANG,[b,c] LING-MING TSENG,[h,i] YI-FANG TSAI,[h] JYH-CHERNG YU,[a,g] ALICE L. YU[a,b,c,j]

[a]Graduate Institute of Life Sciences, National Defense Medical Center, Taipei, Taiwan; [b]Genomics Research Center, Academia Sinica, Taipei, Taiwan; [c]Institute of Stem Cell and Translational Cancer Research, Chang Gung Memorial Hospital at Linkou, Taoyuan, Taiwan; [d]Institute of Cellular and Organismic Biology, Academia Sinica, Taipei, Taiwan; [e]School of Biomedical Sciences, Chung Shan Medical University, Taichung, Taiwan; [f]Department of Medical Research, Chung Shan Medical University Hospital, Taichung, Taiwan; [g]Division of General Surgery, Department of Surgery, Tri-Service General Hospital, Taipei, Taiwan; [h]Division of General Surgery, Department of Surgery, Taipei-Veterans General Hospital, Taipei, Taiwan; [i]National Yang Ming University, Taipei, Taiwan; [j]Department of Pediatrics, University of California in San Diego, San Diego, California, USA

Correspondence: Alice L. Yu, M.D., Ph.D., Institute of Stem Cell and Translational Cancer Research, Chang Gung Memorial Hospital at Linkou and Chang Gung University, No.5, Fusing St., Gueishan Township, Taoyuan 33305, Taiwan. Telephone: 886-3-328-1200, ext 5217; Fax: 886-3-328-1200, ext 5214; e-mail: aliceyu@ucsd.edu; or Jyh-Cherng Yu, M.D., Division of General Surgery, Department of Surgery, Tri-Service General Hospital, 325,Chenggong Road, Section 2, Taipei 114, Taiwan. Telephone: 886-2-8792-7171; Fax: 886-2-8792-7372; e-mail: doc20106@ndmctsgh.edu.tw

Received October 24, 2013; accepted for publication April 9, 2014; first published online in STEM CELLS *EXPRESS* May 6, 2014.

1066-5099/2014/$30.00/0

http://dx.doi.org/10.1002/stem.1735

Key Words. SHIP2 • Breast cancer stem cells • JNK • Vimentin

ABSTRACT

Overexpression of SH2-containing-5′-inositol phosphatase-2 (SHIP2) correlates with poor survival in breast cancer. However, its role in breast cancer stem cells (BCSCs) remains unclear. Here, we showed that the percentage of SHIP2$^+$ cells was positively correlated with that of CD24$^-$CD44$^+$ cells in 60 breast cancer specimens. Among 20 estrogen receptor (ER)-negative samples, 17 had greater SHIP2 expression in CD24$^-$CD44$^+$ subpopulation than the remaining subpopulation. Data mining of microarray analysis of 295 breast tumors showed a significant correlation of higher *SHIP2* expression with distant metastasis. Examination of patient-derived mouse xenografts revealed that SHIP2 protein and its tyrosine 1135 phosphorylation were significantly higher in BCSCs, identified as CD24$^-$CD44$^+$ or aldehyde dehydrogenase (ALDH$^+$), than non-BCSCs. SHIP2 silencing or inhibitor of SHIP2 phosphatase significantly decreased mammosphere-forming efficiency, ALDH$^+$ subpopulation in vitro and tumorigenicity of BCSCs in vivo. Overexpression of SHIP2 enhanced the expression of epithelial–mesenchymal transition markers including vimentin (VIM), which was mainly expressed in ER-negative breast cancer cells with higher level in mammospheres than monolayer culture. Ablation of c-Jun *N*-terminal kinase 1 (JNK1), JNK2, or VIM diminished the increased ALDH$^+$ population and tumorigenicity, induced by SHIP2 overexpression. BCSCs displayed greater expression of phospho-JNK than non-BCSCs and silencing of JNK suppressed SHIP2-mediated upregulation of VIM. Furthermore, SHIP2 overexpression enhanced Akt activation, but Akt inhibition failed to influence SHIP2-induced phospho-JNK/VIM upregulation. In conclusion, SHIP2 plays a key role in BCSCs of ER-negative breast cancers through activation of Akt and JNK with upregulation of VIM and may serve as a target for therapy directed at BCSCs. STEM CELLS *2014;32:2048–2060*

INTRODUCTION

Cancer stem cells (CSCs) have been defined as a small proportion of tumor cells with the capacity for self-renewal, differentiation, and tumorigenicity. It was initially demonstrated in acute myeloid leukemia in 1994 [1]. Since then, CSCs have been identified from several types of solid tumors, including breast, brain, pancreatic, and colon [2–5]. Al-Hajj et al. first identified human breast CSCs (BCSCs) as CD44$^+$CD24$^{-/low}$ cells, and subsequently Ginestier et al. showed that BCSCs were enriched in cells with high activity of aldehyde dehydrogenase 1 (ALDH1) [4, 6]. To date, CSCs have been shown to be responsible for metastasis and resistance to drugs and radiation [7–9]. Thus, identification of suitable target molecules and/or pathways to eradicate CSCs is urgently needed.

In breast cancer, SH2-containing-5′-inositol phosphatase-2 (SHIP2) has been shown to promote cancer cell proliferation and metastasis by interacting with c-cbl to prevent epidermal growth factor (EGF) receptor (EGFR) turnover and enhancing EGF-induced Akt activation [10, 11]. The expression of SHIP2 was higher in breast cancer cells than normal mammary epithelial cells, and immunohistochemical analysis of clinical samples showed that higher level of SHIP2 correlated with shorter survival of patients with invasive breast cancer [12]. However, it remains unclear whether SHIP2 contributes to the features of CSCs, which are important target for cancer therapy.

SHIP2, an inositol phosphatase which converts phosphatidylinositol (3,4,5)-trisphosphate [PI(3,4,5)P3] into phosphatidylinositol (3,4)-biphosphate [PI(3,4)P2], could block insulin-stimulated phosphatidylinositol-3-kinase (PI3K)/Akt activation, while SHIP2 depletion induced proliferation of insulin-producing cells and increased insulin sensitivity [13, 14]. However, blocking of SHIP2 activity by pan-SHIP

inhibitors reduced cell survival in breast cancer cell lines, MDA-MB-231, and MCF7 cells [15]. Independent of its inositol phosphatase activity, SHIP2 has been shown to interact with other proteins through SH2 domain at its N-terminus and a proline-rich C-terminal tail ending with a sterile alpha motif domain, including c-cbl [16, 17], p130Cas [18], filamin [19], vinexin [20], c-Met [21], EphA2 receptor [22, 23], and c-Jun *N*-terminal kinase 1 (JNK)-interacting protein 1 (JIP1) [24]. These findings suggest that SHIP2 may exert diverse biological functions independent of its phosphatase activity.

In this study, we showed that higher SHIP2 expression in primary human breast cancer specimens positively correlated with the greater percentage of $CD24^-CD44^+$ subpopulation, and a greater SHIP2 expression in $CD24^-CD44^+$ than non-$CD24^-CD44^+$ cells was observed in estrogen receptor (ER)-negative breast cancer. Furthermore, we demonstrated that SHIP2 played an essential oncogenic role for the maintenance of BCSC subpopulation, the mammosphere-forming ability in vitro and tumorigenicity in vivo through JNK/vimentin (VIM) activation.

Materials and Methods

Primary Tumor Cell Isolation and Transplantation

Human clinical breast cancer specimens were obtained from patients at the time of initial surgery and were fully encoded to protect patient confidentiality. Clinical specimens were utilized under a protocol approved by the Institutional Review Board of the Human Subjects Research Ethics Committee of Academia Sinica, Tri-Service General Hospital and Veterans General Hospital (Taipei, Taiwan). Isolation of the primary tumor cells from clinical specimens were described previously [25]. Briefly, the tumor specimens were enzymatically digested by incubation with collagenase, hyaluronidase, and DNase I. Tumor cells were filtrated through a 100-μm cell strainer and separated from red blood cells and dead cells by Percoll density gradient centrifugation. The buffy coat was washed and resuspended for inoculation or flow cytometric analysis. To establish mouse-engrafted tumors, the tumor cells mixed with normal human mammary fibroblasts and Matrigel (BD biosciences, San Jose, CA, http://www.bdbiosciences.com) were subcutaneously injected into mammary fat pads of 8–12-week-old female nonobese diabetic/severe combined immunodeficient (NOD/SCID) mice, purchased from Tzu Chi University (Hualien, Taiwan) and Jackson Laboratory (West Grove, PA, http://www.jax.org). The protocol for animal experimentation was approved by the Institutional Animal Care and Utilization Committee of Academia Sinica, Taipei, Taiwan. Four xenografts were successfully established from patients BC0145, BC0244, BC0350, and BC0634, and their clinical pathological features were shown in Supporting Information Table S1. BCSC subpopulation was delineated as $CD24^-CD44^+$ cells in BC0145, and $ALDH^+$ cells in BC0244, BC350, and BC0634, according to their tumorigenicity [26].

Cell Culture, Cell Viability Determination, and Reagents

Monolayer cultures of H-$2K^{d-}CD24^-CD44^+$ of BC0145, H-$2K^{d-}ALDH^+$ of BC0244, and H-$2K^{d-}$ of BC0634 sorted from xenograft tumors of human primary breast cancer (Supporting Information Table S1) were designated as AS-B145, AS-B244, and AS-B634 cells, respectively, as described previously [26]. These cells as well as MCF7 and ZR75-1 were cultured in minimum essential medium containing 10% fetal bovine serum (FBS), 1 mM sodium pyruvate, 2 mM GlutaMAX, and 10 μg/ml insulin. MDA-MB-231 cells were cultured in Dulbecco's modified Eagle's medium (DMEM) containing 10% FBS; T47D and BT483 cells were cultured in RPMI-1640 containing 10% FBS. MCF10A cell line was obtained from ATCC, and cultured in mammary epithelial basal medium containing 5% FBS, 10 ng/ml EGF, 5 μg/ml insulin, and 0.5 μg/ml hydrocortisone. All the cells were maintained at 37°C with 5% CO_2 in air atmosphere. Cell viability was determined by incubation with 10% AlamarBlue reagent (Biosource International, Camarillo, CA, http://www.lifetechnologies.com) for 2 hours, followed by measurement of fluorescence with excitation at 544 nm and emission at 590 nm using a spectrophotometer (Spectramax 190, Molecular Devices, Sunnyvale, CA, http://www.moleculardevices.com/). The SHIP2-selective competitive inhibitor (AS1938909) [27] and JNK inhibitor II (SP600125) were obtained from Merck-Calbiochem (San Diego, CA, http://www.merckmillipore.com). PI(3,4)P2-diC16 was purchased from Echelon Biosciences Inc. (Salt lake city, UT, http://www.echelon-inc.com). Akt1/2 kinase inhibitor was obtained from Sigma-Aldrich (St. Louis, MO, http://www.sigmaaldrich.com).

Plasmids and Lentiviruses

All lentiviral short hairpin RNA (shRNA) plasmids listed in Supporting Information Table S2 were purchased from National RNAi Core Facility of the Institute of Molecular Biology/Genomics Research Center, Academia Sinica, supported by the National Research Program for Genomic Medicine grants of the National Science Council, Taiwan (NSC 100-2319-B-001-002). The shRNA plasmid against luciferase served as negative control (sh-Ctrl) in all knocking down experiments. For plasmid construction, full-length coding sequences of human SHIP2 (INPPL1, accession number NM_001567) were cloned with specific primers (forward: CCCGCTAGCATGGCCTCGGCCTGCGGG, reverse: CCCGAATTCTCA CTTGCTGAGCTGCAGGGTG) into pLKO AS2.puro vector (National RNAi Core Facility). The procedure for lentiviruses production was described previously [25]. Cells were infected by viruses at a multiplicity of infection (MOI) of 1–5 with the addition of 8 μg/ml polybrene (Sigma-Aldrich). AS-B634 cells were transduced by lentiviruses carrying vector overexpressing SHIP2 or control vector and selected by 2 μg/ml puromycin (Sigma-Aldrich) for more than 1 month to generate stable clones of puromycin-resistant cells.

Fluorescence-Activated Cell Sorting

For SHIP2 immunostaining, 2.5–5.0 $\times$ 10^5 cells isolated from primary tumors were fixed at 37°C for 10 minutes with BD Phosflow fix buffer and preserved at −80°C for batch analysis. After thawing and washing, the fixed cells were permealized with BD Phosflow Perm Buffer III on ice for 30 minutes and stained for another 30 minutes with anti-human SHIP2 rabbit monoclonal antibodies or isotype control rabbit monoclonal IgG (Cell Signaling Technology, Danvers, MA, http://www.cellsignal.com), Alexa Fluor 488-goat anti-rabbit IgG (Invitrogen, Life Technologies, Inc., Grand Island, NY, http://www.invitrogen.com), and anti-CD24-PE, anti-CD44-APC, and

anti-CD45-PE-Cy7 antibodies (BD biosciences). Cells were then washed with phosphate-buffered saline (PBS) and analyzed by flow cytometric analyses using BD Diva software and a BD FACSCanto II flow cytometer. The percentage of SHIP2$^+$ cells was determined by FCS Express software after subtraction of isotype control. ALDEFLUOR assay (StemCell Technologies, Vancouver, Canada, http://www.stemcell.com) was performed according to the manufacturer's recommendations. Briefly, 1 $\times$ 10^5 cells were suspended in 100 μl of assay buffer and incubated with BODIPY-aminoacetaldehyde substrate and/or 150 μM diethylaminobenzaldehyde (DEAB) at 37°C for 30 minutes and further stained with 7-AAD on ice for 10 minutes. After washing, cells were analyzed by flow cytometry and gated into ALDH$^+$ and ALDH$^-$ cells of viable cells (7AAD$^-$). For sorting of ALDH$^+$ and ALDH$^-$ subpopulation, cells were first stained with ALDEFLUOR kit, followed by anti-H2K^d–APC and then 7-AAD. For sorting of CD24$^-$CD44$^+$ and the remaining subpopulation, cells were first stained with anti-CD24-PE, anti-CD44-APC, and anti-H2k^d-FITC, followed by 7-AAD. Cell sorting was carried out on a FACSAria cell sorter (BD Biosciences).

Real-Time Quantitative PCR

RNAs were extracted using the TRIzol Reagent (Invitrogen). cDNA was synthesized by a SuperScript III First-Strand Synthesis kit (Invitrogen). cDNAs of 5–10 ng was used for SYBR Green quantitative polymerase chain reaction (qPCR) analysis. The sequences of qPCR primers for JNK1, JNK2, SHIP2, GAPDH, E-cadherin, VIM, N-cadherin, fibronectin 1 (FN1), and Slug, provided on the Web site of Origene, Inc. (Rockville, MD, http://www.origene.com), were listed in Supporting Information Table S3. SYBR Green master mix reagents were obtained from Roche Diagnostics Corp. (Indianapolis, Indiana, http://www.roche-diagnostics.us). qPCR assays were performed on the Real-Time PCR 7300 system or StepOne Plus real-time PCR system (Applied Biosystems, Foster City, CA, http://www.appliedbiosystems.com).

Western Blotting

Cells were washed with PBS and lysed in RIPA buffer containing NP-40, protease inhibitors (Roche), and tyrosine and serine/threonine phosphatase inhibitors (Sigma-Aldrich). Total protein extracts of 10–30 μg were separated on 4–12% NuPAGE (Invitrogen) and transferred to polyvinylidene difluoride membranes (Millipore, Bedford, MA, https://www.millipore.com). The membranes were incubated with primary antibodies at 4°C overnight followed by alkaline phosphatase-conjugated secondary antibodies (Jackson Immunoresearch Laboratories, West Grove, PA, http://www.jacksonimmuno.com) at room temperature for 1 hour. Then, the membrane was scanned by a Typhoon9400 Variable Mode Imager (GE Healthcare Life Sciences, Uppsala, Sweden, http://www.gelifesciences.com) to detect the fluorescent signals released from catalyzed ECF substrate (GE Healthcare). Antibodies against SHIP2, phospho-SHIP2 ^{Tyr1135}, phospho-JNK$^{Thr183/Tyr185}$, phosphor-Akt^{Ser473}, phospho-Akt^{Thr308}, Akt, and GAPDH were purchased from Cell Signaling Technology, and those against JNK and VIM were obtained from Santa Cruz Biotechnology (Santa Cruz, CA, http://www.scbt.com). Anti-α-tubulin antibody was purchased from Sigma-Aldrich. Anti-FN1 antibody was obtained from Millipore. Anti-Slug antibody was purchased from Abcam Inc., Cambridge, MA, http://www.abcam.com. The results of Western blots were quantified by ImageQuant 5.2 software (GE Healthcare).

Mammosphere Formation Assay

Cultured cells were trypsinized and seeded at 500 or 1000 cells per well into 96-well low-attachment plates (Corning Inc., Corning, NY, http://www.corning.com) and cultured in DMEM-F12 medium (Lonza Walkersville Inc., Walkersville, MD, http://www.lonza.com) containing 0.4% bovine serum albumin, 20 ng/ml basic fibroblast growth factor (PeproTech, Rocky Hill, NJ, http://www.peprotech.com), 20 ng/ml EGF (PeproTech), 5 μg/ml insulin, and B27 supplement (Life Technologies Inc.). At 7–15 days, the number of mammospheres greater than 50 μm diameter was counted under an inverted microscope. Mammosphere-forming efficiency (MFE, %) was calculated as follows [28]: (number of mammospheres per well/number of cells seeded per well) $\times$ 100

Tumorigenicity In Vivo

BC0145-CSC (CD24$^-$CD44$^+$) and BC0244-CSC (ALDH$^+$) cells were sorted as described previously from xenograft tumors and cultured overnight, followed by infection with lentiviral shRNAs for 3 days. The viable puromycin-resistant cells were trypsinized and mixed with human normal mammary fibroblasts and Matrigel for subcutaneous injection into the mammary fat pads of NOD/SCID mice. Tumor formation was monitored weekly after inoculation. The frequency of tumor-initiating cell (TIC) was calculated by Extreme Limiting Dilution Analysis software [29]. To assess the in vivo effect of SHIP2 inhibitor, AS1938909, mice were treated with the inhibitor intravenously twice per week for 4 weeks, starting at 4 days after tumor inoculation.

Statistical Analysis

Correlation analyses of clinical characteristics except breast cancer subtypes shown in tables were determined by Fisher's exact test. The correlation of subtypes was analyzed by Chi-square test. Data presented as mean $\pm$ SD were analyzed by Student's *t*-test. $p < .05$ was considered as significant.

Results

Increased SHIP2 Expression in BCSCs of ER-Negative Breast Cancers

To evaluate the role of SHIP2 in BCSCs, we first examined the expression of SHIP2 in BCSC and non-BCSC subpopulations in clinical specimens obtained from 60 breast cancer patients whose clinical pathological characteristics were summarized in Supporting Information Table S4. The expression levels of SHIP2 in both non-BCSCs (non-CD24$^-$CD44$^+$) and BCSCs (CD24$^-$CD44$^+$) of freshly isolated breast cancer cells (CD45$^-$) were determined by flow cytometry. Figure 1A showed the analysis of a representative sample. Among 60 specimens investigated (Fig. 1B), the percentage of SHIP2$^+$ cells was positively correlated with that of CD24$^-$CD44$^+$ cells within total tumor cells (Spearman $r = .3$, $p = .02$). In 5 of 60 specimens, SHIP2 was not detectable, and 13 of 60 showed no discernible CD24$^-$CD44$^+$ cells by flow cytometry (Supporting Information Table S5).

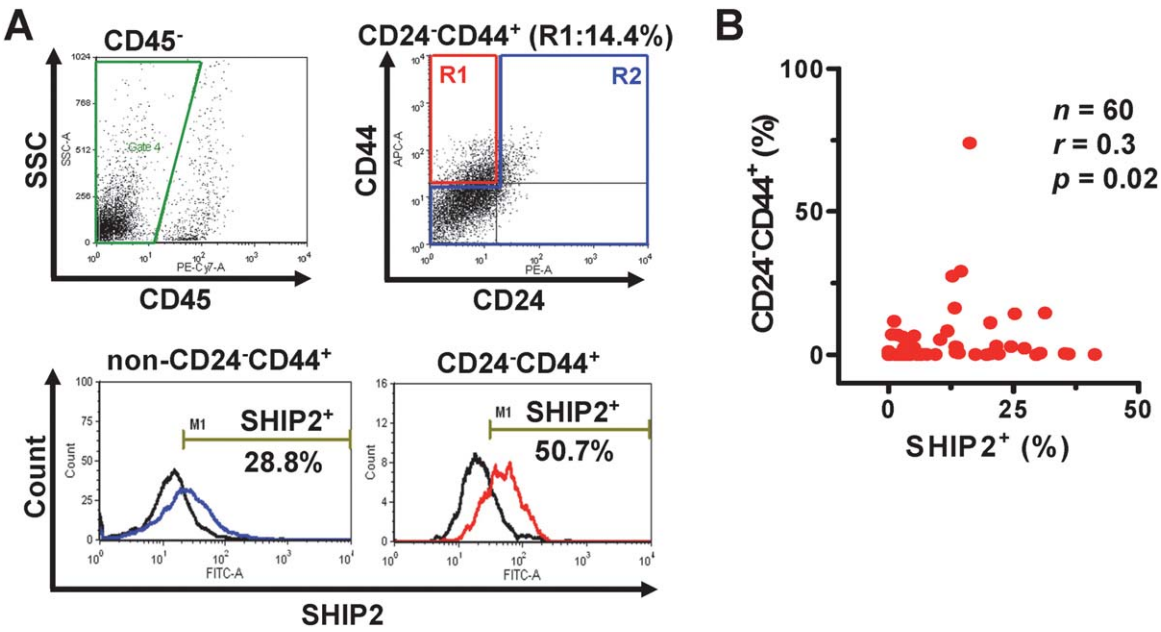

Figure 1. Flow cytometric analysis of SH2-containing-5′-inositol phosphatase-2 (SHIP2) expression in $CD24^{-}CD44^{+}$ and non-$CD24^{-}CD44^{+}$ populations from primary human breast cancer cells. Breast cancer cells harvested from clinical breast cancer specimens were stained with fluorescence-conjugated antibodies and detected by flow cytometry. **(A):** A representative sample, BC1126, of 60 clinical specimens examined was shown. BC1126 was a 50-year old patient with stage IIIA, ER^{+}, PR^{+}, $Her2^{-}$ lobular carcinoma. Tumor cells were first gated on $CD45^{-}$ population to exclude leukocytes (upper left panel). Among $CD45^{-}$ tumor cells, $CD24^{-}CD44^{+}$ subpopulation in region R1 and the remaining non-$CD24^{-}CD44^{+}$ cells in region R2 were shown (upper right panel). The SHIP2 expression levels of non-$CD24^{-}CD44^{+}$ subpopulation (blue) and $CD24^{-}CD44^{+}$ subpopulation (red) were normalized to its own isotype control (black) (lower panel). **(B):** The dot plots showed the correlation of percentages (%) of $SHIP2^{+}$ cells and $CD24^{-}CD44^{+}$ cells in each tumor among 60 (*n*) clinical specimens. The *r* and *p* values were calculated by Spearman's rank correlation analysis. Abbreviations: SHIP2, SH2-containing-5′-inositol phosphatase-2; SSC, side scatter.

Next, we analyzed whether the expression level of SHIP2 in total tumor cells correlated with clinical parameters. As shown in Supporting Information Table S4, there was a trend for lymph node involvement in SHIP2 high expression group (>4%) ($p = .07$). Moreover, data mining of microarray analysis of 295 clinical breast cancer specimens reported by van de Vijver et al. [30] revealed a significant correlation of greater SHIP2 expression with distant metastasis (Supporting Information Table S6, $p = .002$). We next compared the SHIP2 expression in BCSCs versus non-BCSCs. Among 44 of 60 samples in which both SHIP2 and $CD24^{-}CD44^{+}$ cells were detectable (Supporting Information Table S5), SHIP2 expression was higher in BCSCs than non-BCSCs in 28 cases (Supporting Information Table S7). There was a significant correlation of ER status with SHIP2 expression in BCSCs. In 20 ER-negative patients, 17 (85.0 %) showed greater expression of SHIP2 in BCSCs than non-BCSCs, whereas 13 of 24 (54.2 %) ER-positive patients displayed equal or higher SHIP2 in non-BCSCs than BCSCs ($p = .01$). No correlation was found with other clinical parameters including age, tumor size, histology grade, stage, lymph node involvement, progesterone receptor, v-erb-b2 avian erythroblastic leukemia viral oncogene homolog 2 (HER2) status, and four molecular subtypes of breast cancer. We further determined SHIP2 expression in BCSCs ($CD24^{-}CD44^{+}$ or $ALDH^{+}$) and paired non-BCSCs ($CD24^{-}CD44^{-/low}$ or $ALDH^{-}$) sorted from four mouse xenografts of primary human ER-negative breast cancer as described in Materials and Methods section. As shown in Figure 2, BCSCs displayed greater expression of SHIP2 protein and its phosphorylation on tyrosine 1135 site than non-BCSCs. Taken together, SHIP2 expression positively correlated with distant metastasis, and BCSCs had higher expression of SHIP2 than non-BCSCs in some subtypes of breast cancer such as ER-negative breast cancers. These results suggested that SHIP2 might play an important role in the tumorigenicity and progression of breast cancer.

SHIP2 Expression Modulates $ALDH^{+}$ Subpopulation and Mammosphere Formation In Vitro and Tumorigenicity In Vivo

AS-B145, AS-B244, or AS-B634 cells, which were derived from xenograft tumors of BC0145, BC0244, or BC0634, respectively, could be propagated as monolayer cultures. They contained $CD24^{-}CD44^{+}$ and $ALDH^{+}$ subpopulation (Supporting Information Fig. S1) and formed mammospheres in vitro (Fig. 3A). To delineate the role of SHIP2 in breast cancer tumorigenicity, we delivered lentiviral shRNAs to knock down SHIP2 expression in AS-B145 and AS-B244 cells. As shown in Figure 3B, 4 days after lentiviral transduction of AS-B145 cells with two different shRNAs (sh-S-1 and sh-S-2), SHIP2 was repressed to 50% of negative control. BCSC subpopulation as characterized by high $ALDH^{+}$ activity was significantly reduced in sh-S-1 and −2 cells to ~0.4 and 0.5- to 0.8-fold of sh-Ctrl cells for AS-B145 and AS-B244, respectively. On the other hand, AS-B634 cells over-expressing SHIP2 showed 3.2- ± 0.4-fold increase in $ALDH^{+}$ subpopulation, while SHIP2 expression level was elevated to 2.0-fold as compared to vector control (Fig. 3C). These results indicated that SHIP2 was important for the

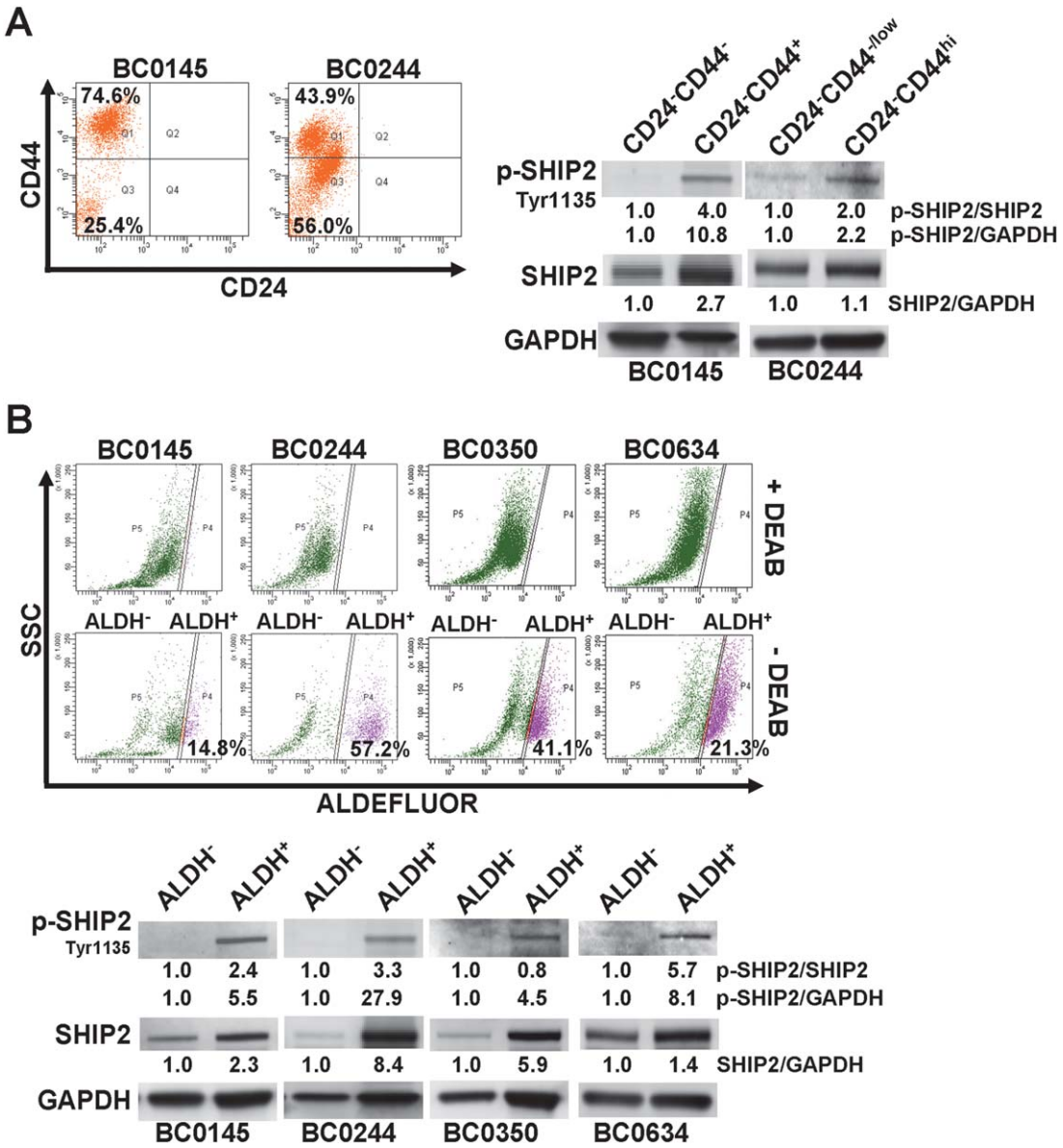

Figure 2. Higher expression and phosphorylation of SH2-containing-5′-inositol phosphatase-2 (SHIP2) in the breast cancer stem cell (BCSC) subpopulation than non-BCSC isolated from xenografts of primary human breast cancer. **(A, B):** Fresh tumor cells were isolated from xenografts of four primary human breast cancer specimens in nonobese diabetic/severe combined immunodeficient mice for fluorescence-activated cell sorting analysis. The viable human cells (7-AAD$^-$H-2K^{d-}) were gated to identify the BCSC subpopulations as CD24$^-$CD44$^+$ or aldehyde dehydrogenase (ALDH$^+$) cells. Diethylaminobenzaldehyde, the inhibitor of ALDH, was used to distinguish ALDH$^+$ (purple) from ALDH$^-$ (green) cells. The expression of SHIP2 and phospho-SHIP2 (Tyr1135) in the subpopulations of CD24$^-$CD44$^{+/hi}$ or CD24$^-$CD44$^{-/low}$ and ALDH$^+$ or ALDH$^-$ was determined by Western blot and presented as fold change. Abbreviations: GAPDH, glyceraldehyde 3-phosphate dehydrogenase; SHIP2, SH2-containing-5′-inositol phosphatase-2; SSC, side scatter.

maintenance of ALDH$^+$ subpopulation. We next assessed the role of SHIP2 in mammosphere-forming ability of BCSCs. As shown in Supporting Information Figure S2, the expression of SHIP2 and phospho-SHIP2$^{Tyr\ 1135}$ was slightly greater in mammosphere than adherent monolayer culture. Silencing of SHIP2 reduced the mammosphere-forming efficiency (MFE) of AS-B145 cells from 4.63 ± 0.47% (sh-Ctrl) to 3.2 ± 0.4% (sh-S-1, $p = .02$) and 3.6 ± 0.2% (sh-S-2, $p = .03$). Similar results were obtained in AS-B244 cells with a significant decrease in MFE from 1.1 ± 0.1% (sh-Ctrl) to 0.2 ± 0.1% (sh-S-1, $p < .001$) and 0.7 ± 0.2% (sh-S-2, $p = .003$) (Fig. 3D). On the other hand, the later passage of SHIP2-overexpressing AS-B634 cells, which had a 7.4-fold increase of SHIP2 expression as compared to 2.0-fold in early passage, exhibited elevated MFE from 0.7 ± 0.1% to 3.3 ± 0.3% ($p = .035$, Fig. 3E). To verify the essential role of SHIP2 in vivo, SHIP2 was silenced by lentiviral shRNAs in BC0145-CSC (CD24$^-$CD44$^+$) sorted from BC0145 xenograft and BC0244-CSC (ALDH$^+$) sorted from BC0244 xenograft. Table 1 showed that the TIC frequency of sh-SHIP2 (sh-S-2) cells as compared to sh-Ctrl cells was significantly decreased from 1:12,509 to 1:104,672 for BC0145-CSC and from 1:3,477 to 1:438,624 for BC0244-CSC. Whereas, SHIP2-overexpressing AS-B634 stable clone increased TIC frequency from 1:56,160 to 1:229 with faster engraftment than

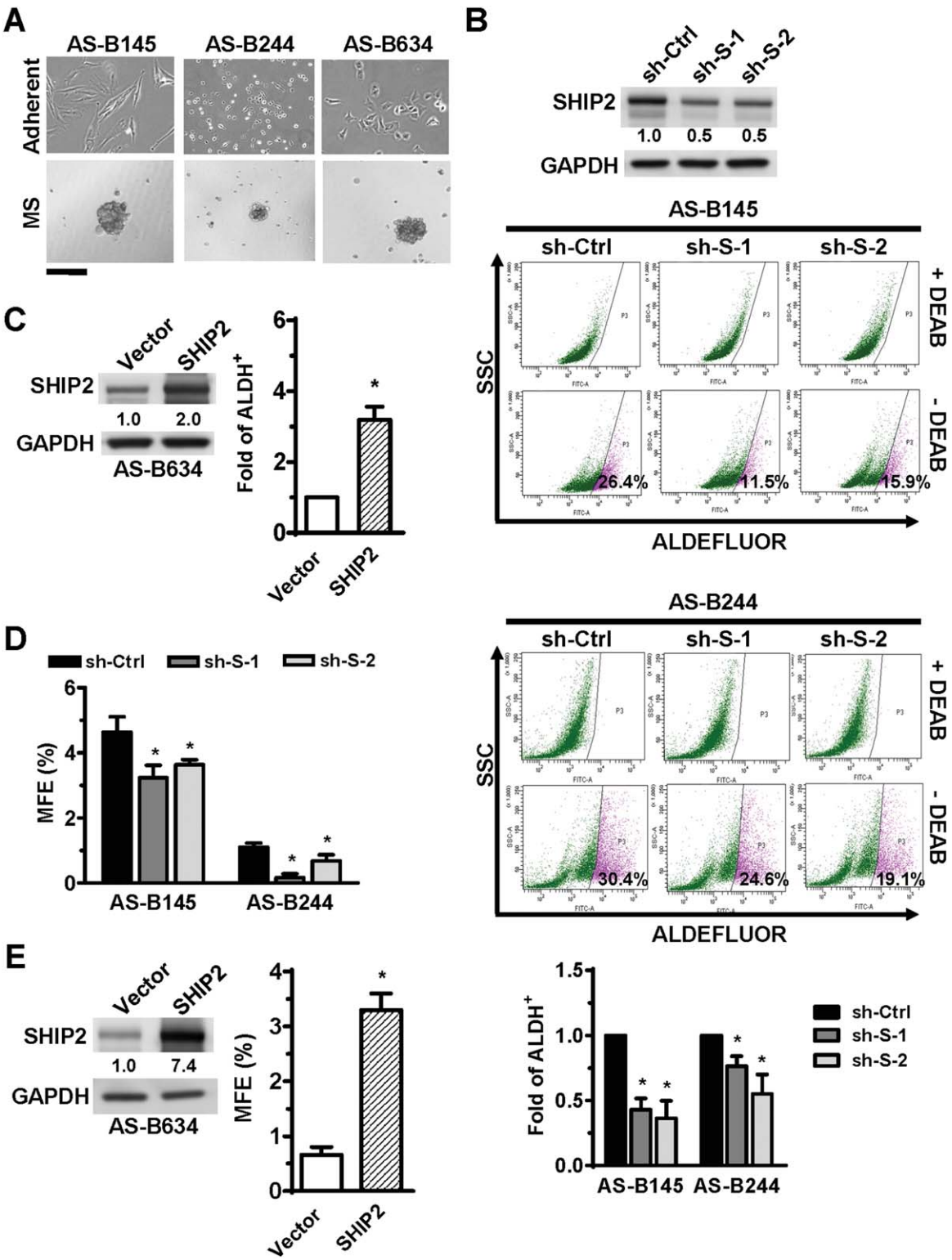

Figure 3. SH2-containing-5′-inositol phosphatase-2 (SHIP2) expression expands the subpopulation of aldehyde dehydrogenase ($ALDH^+$) cells and enhances mammosphere (MS) formation. **(A):** AS-B145, AS-B244, or AS-B634 cells were cultured in adherent monolayer or MS condition as described in Materials and Methods section. The pictures were taken under microscope. Scale bar = 200 μm. **(B, D):** AS-B145 cells were transduced with shRNAs to knock down SHIP2 (sh-S-1, −2). Sh-Ctrl was a negative control shRNA. Four days after transfection, the expression of SHIP2 was determined by Western blot. Four days after transduction of AS-B145 or AS-B244 cells with lentiviral shRNAs targeting SHIP2, the percentage of $ALDH^+$ subpopulation was determined by flow cytometry and MS-forming efficiency (MFE) was calculated. Fluorescence-activated cell sorting plots were representative of three independent experiments. **(C):** The expression level of SHIP2 in SHIP2-overexpressing AS-B634 cells was shown, and their $ALDH^+$ subpopulation was determined. **(E):** The expression level of SHIP2 in SHIP2-overexpressing stable clone of AS-B634 was shown, and their MFE were determined. Data were shown as Mean ± SD. *, $p < .05$. Abbreviations: DEAB, diethylaminobenzaldehyde; MFE, MS-forming efficiency; MS, mammosphere; SHIP2, SH2-containing-5′-inositol phosphatase-2; shRNA, short hairpin RNA.

Table 1. Tumorigenicity of cells after silencing or overexpressing SHIP2

Cell treatment	Injected cell number					TIC Frequency	*p*
BC0145-CSC	1.5×10^5	3.0×10^4	3.0×10^3				0.005
sh-Ctrl	7/7	4/4	0/4			1:12,509	
sh-S-2	6/7	0/4	0/4			1:104,672	
BC0244-CSC	1.0×10^5	7.0×10^4	1.0×10^3				$<<$0.001
sh-Ctrl	11/11	3/3	1/4			1:3,477	
sh-S-2	0/11	0/3	0/4			$<$1: 438,624	
AS-B634	10^5	10^4	10^3	10^2	10^1		$<<$0.001
Vector	4/6	3/6	0/5	ND	ND	1:56,160	
SHIP2	6/6	6/6	5/6	4/6	2/6	1:229	

The TIC frequency was calculated by ELDA software. ND, not determined.

vector control. These results indicated that SHIP2 contributed to maintaining the properties of breast CSCs.

SHIP2 Phosphatase Activity Modulates ALDH$^+$ Subpopulation and Mammosphere Formation In Vitro and Tumorigenicity In Vivo

To delineate the role of phosphatase activity of SHIP2 in breast CSCs, we analyzed the effects of a SHIP2-selective competitive inhibitor, AS1938909, in SHIP2-overexpressing AS-B634 stable clone. As shown in Figure 4A, treatment with SHIP2 inhibitor for 4 days decreased cell viability to 70.0 $\pm$ 6.5% or 47.3 $\pm$ 4.4% of dimethyl sulfoxide (DMSO) control at 25 μM, and 34.5 $\pm$ 4.4% or 1.8 $\pm$ 0.3% at 50 μM in SHIP2-overexpressing AS-B634 or vector control cells, respectively. As expected, SHIP2-overexpressing cells were less sensitive to the inhibitor than the vector control cells. Furthermore, BCSC subpopulation identified as ALDH$^+$ cells in SHIP2-overexpressing AS-B634 was reduced to 0.5- $\pm$ 0.2-fold at 25 μM and 0.3- $\pm$ 0.02-fold at 50 μM (Fig. 4B; Supporting Information Fig. S3), along with decreased MFE of SHIP2-overexpressing AS-B634 from 3.3 $\pm$ 0.3% (DMSO control) to 0.2 $\pm$ 0.1% at 25 μM and 0% at 50 μM (Fig. 4C). Moreover, SHIP2 phosphatase inhibitor reduced the tumor volume engrafted by SHIP2-overexpressing AS-B634 cells from 1.4 $\pm$ 0.4 cm^3 (DMSO) and 1.2 $\pm$ 0.3 cm^3 (untreated control) to 0.5 $\pm$ 0.3 cm^3 in vivo ($p = .01$, Fig. 4D). As showed in Figure 4E, both SHIP2 shRNA knockdown and SHIP2 phosphatase inhibitor in SHIP2-overexpressing AS-B634 cells suppressed p-Akt^{Ser473} levels. Furthermore, regulation of Ser473 and Thr308 phosphorylation on Akt by SHIP2 was also observed in breast cancer cells not overexpressing SHIP2, such as AS-B634 (Supporting Information Fig. S4). Next, we delivered the product of SHIP2 phosphatase, PI(3,4)P2, to rescue SHIP2-overexpressing AS-B634 cells from the effects of SHIP2 phosphatase inhibitor. As showed in Figure 4E, addition of PI(3,4)P2 could partially rescue Akt phosphorylation from 0.6- to 0.8-fold and ALDH$^+$ subpopulation from 0.46- $\pm$ 0.05-fold to 0.72- $\pm$ 0.04-fold in SHIP2-overexpressing AS-B634 cells treated with SHIP2 phosphatase inhibitor ($p = .03$, Fig. 4F), whereas PI(3,4)P2 failed to reverse the effects of SHIP2-silencing on Akt activation (Fig. 4E) and ALDH$^+$ subpopulation (Fig. 4G). These results demonstrated that the oncogenic role of SHIP2 in breast cancer might be attributed partially, but not entirely to its phosphatase activity.

SHIP2 Positively Regulates Vimentin Expression in ER-Negative Breast Cancers

In light of our finding that SHIP2 significantly correlated with metastasis, we investigated the possible involvement of SHIP2 in epithelial–mesenchymal transition (EMT). As shown in Figure 5A, the stable clone of SHIP2-overexpressing ASB634 cells harbored significantly lower levels of E-cadherin, and higher levels of N-cadherin, FN1, Slug, and VIM than control cells. On the other hand, SHIP2 knockdown in MDA-MB-231 cells to 0.4 $\pm$ 0.1 and 0.3- $\pm$ 0.04-fold by sh-S-1 and sh-S-2, respectively, reduced the expression of *VIM* to 0.5- $\pm$ 0.03-fold ($p = .001$) and 0.4- $\pm$ 0.1-fold ($p = .005$) at mRNA level, and 0.6- and 0.4-fold at protein level, respectively, although the expression of *N-cadherin*, *Slug* and *FN1* was not affected (Fig. 5B). Similarly, SHIP2 silencing in AS-B145 and AS-B244 cells reduced the mRNA level of *VIM* to 0.6- $\pm$ 0.03-fold and 0.4- $\pm$ 0.2-fold, respectively (Fig. 5C), and decreased the protein level of VIM to 0.6-fold in AS-B145 cells (Supporting Information Fig. S5A). Furthermore, treatment with inhibitor of SHIP2 phosphatase at 50 μM diminished the expression of *VIM* from 2.32- $\pm$ 0.16-fold to 0.81- $\pm$ 0.03-fold increase in SHIP2-overexpressing AS-B634 cells, as compared to vector control cells ($p < .001$, Supporting Information Fig. S6). Since VIM expression was reported to be greater in breast cancer samples with higher percentage ($\geq$ 10%) of CD24$^{-/low}$CD44$^+$ cells [31], we examined the relationship between SHIP2 and VIM. In view of a significant correlation of ER-negative status with higher SHIP2 expression in CD24$^-$CD44$^+$ cells than non-CD24$^-$CD44$^+$ cells, we determined VIM expression in ER-negative and ER-positive breast cancer cell lines. As shown in Figure 5D, ER-negative cell lines, MCF10A, MDA-MB-231, or cells cultured from xenografts including AS-B145, AS-B244 and AS-B634 expressed VIM, while no VIM expression was detected in all ER-positive breast cancer cell lines tested including T47D, ZR75-1, BT483, and MCF7. Moreover, VIM expression in mammospheres of AS-B145 and AS-B634 cells was 1.6- to 3.5-fold greater than adherent monolayer cultures (Fig. 5E). On the other hand, BCSCs derived from mouse xenografts of BC0145 and BC0244 had higher expression (4.4- to 6.3-fold) of VIM proteins than paired non-BCSCs (Supporting Information Fig. S5B). Hence, we determined whether VIM indeed contributed to the maintenance of BCSCs. As shown in Figure 5F, knockdown of VIM by shRNAs to 0.3- $\pm$ 0.2-fold (sh-VIM-1) and 0.1- $\pm$ 0.1-fold (sh-VIM-2) in AS-B145 cells significantly reduced the ALDH$^+$ subpopulation to 0.76- $\pm$ 0.06-fold and 0.46- $\pm$ 0.16-fold, and the CD24$^-$CD44$^+$ subpopulation to 0.55- $\pm$ 0.08-fold and 0.37- $\pm$ 0.04-fold, respectively. These findings suggested that the importance of SHIP2 in BCSCs of ER-negative breast cancers might in part be attributed to its upregulation of VIM expression.

SHIP2 Induces Vimentin Expression Through JNK Activation

To further investigate the molecular mechanism of SHIP2-mediated VIM upregulation, we examined a potential candidate

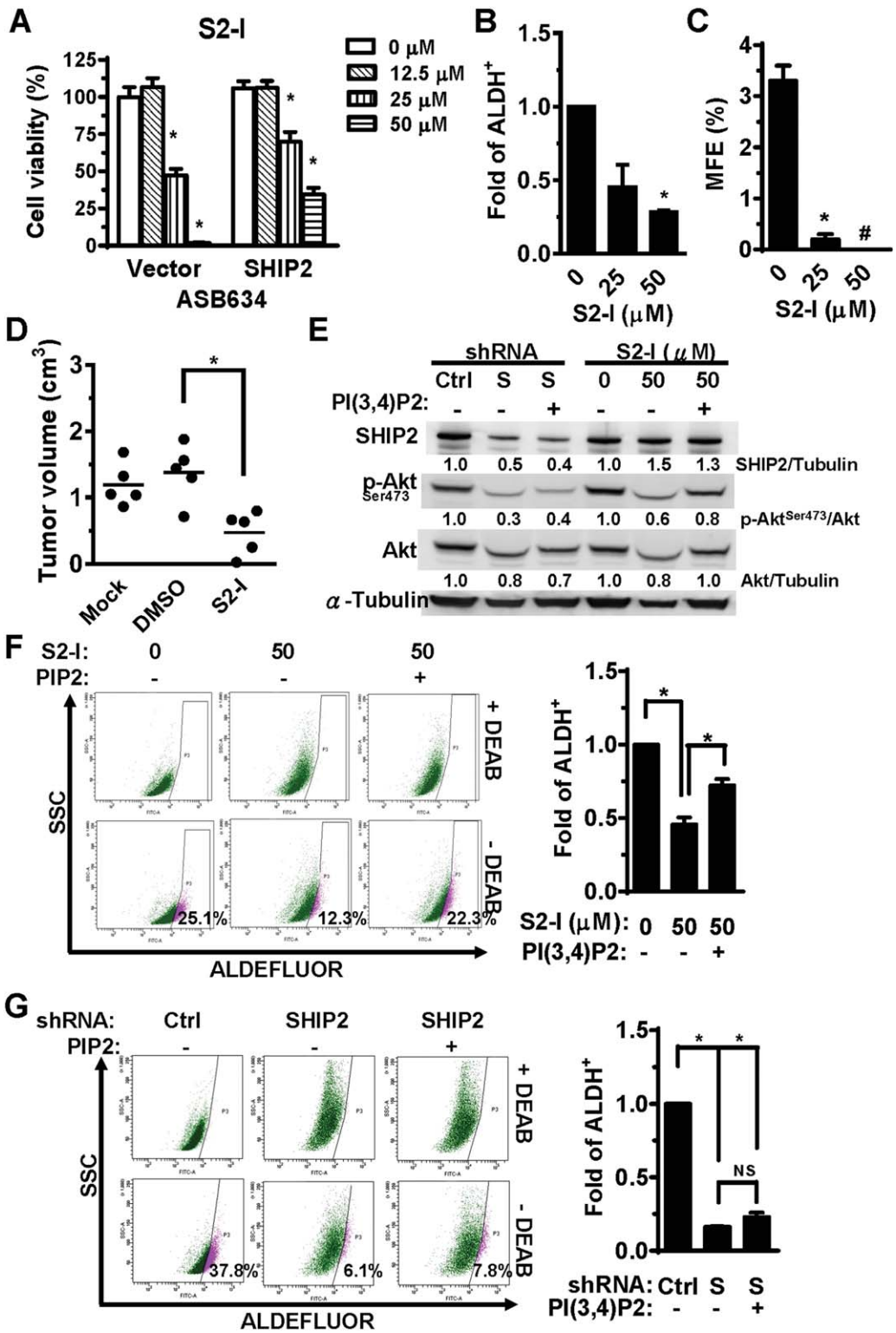

Figure 4. Inhibition of SH2-containing-5′-inositol phosphatase-2 (SHIP2) phosphatase activity reduces aldehyde dehydrogenase ($ALDH^+$) population and mammosphere (MS) formation in vitro and impairs tumorigenicity in vivo. **(A):** The viability of AS-B634 cells (vector control and SHIP2-overexpressing groups) after treatment with SHIP2 inhibitor (S2-I) at the indicated concentration for 4 days was determined by AlamarBlue reagents. **(B, C):** After incubation with SHIP2 inhibitor, the percentage of $ALDH^+$ population and MS-forming efficiency (MFE) of ASB634 SHIP2-overexpressing stable clone were determined. #, no MS was observed. **(D):** The tumor volume of AS-B634 SHIP2-overexpressing stable clone on day 28 after treatment with DMSO or 50 μM SHIP2 inhibitor (S2-I) or untreated control (Mock) was determined as described in Materials and Methods section. **(E):** The protein levels of SHIP2, phospho-Akt, or Akt in SHIP2-overexpressing AS-B634 stable clone were determined by Western blots 3 days after SHIP2 shRNA knockdown (S) or SHIP2 phosphatase inhibition (S2-I) with or without the addition of 25 μM PI(3,4)P2 for the last 2 days, and **(F, G)** the percentage of their $ALDH^+$ population was determined. Representative fluorescence-activated cell sorting plots of two independent experiments were shown. Data were shown as mean $\pm$ SD. *, $p < .05$. Abbreviations: DEAB, diethylaminobenzaldehyde; DMSO, dimethyl sulfoxide; MFE, mammosphere-forming efficiency; NS, not significant; SHIP2, SH2-containing-5′-inositol phosphatase-2; shRNA, short hairpin RNA; SSC, side scatter.

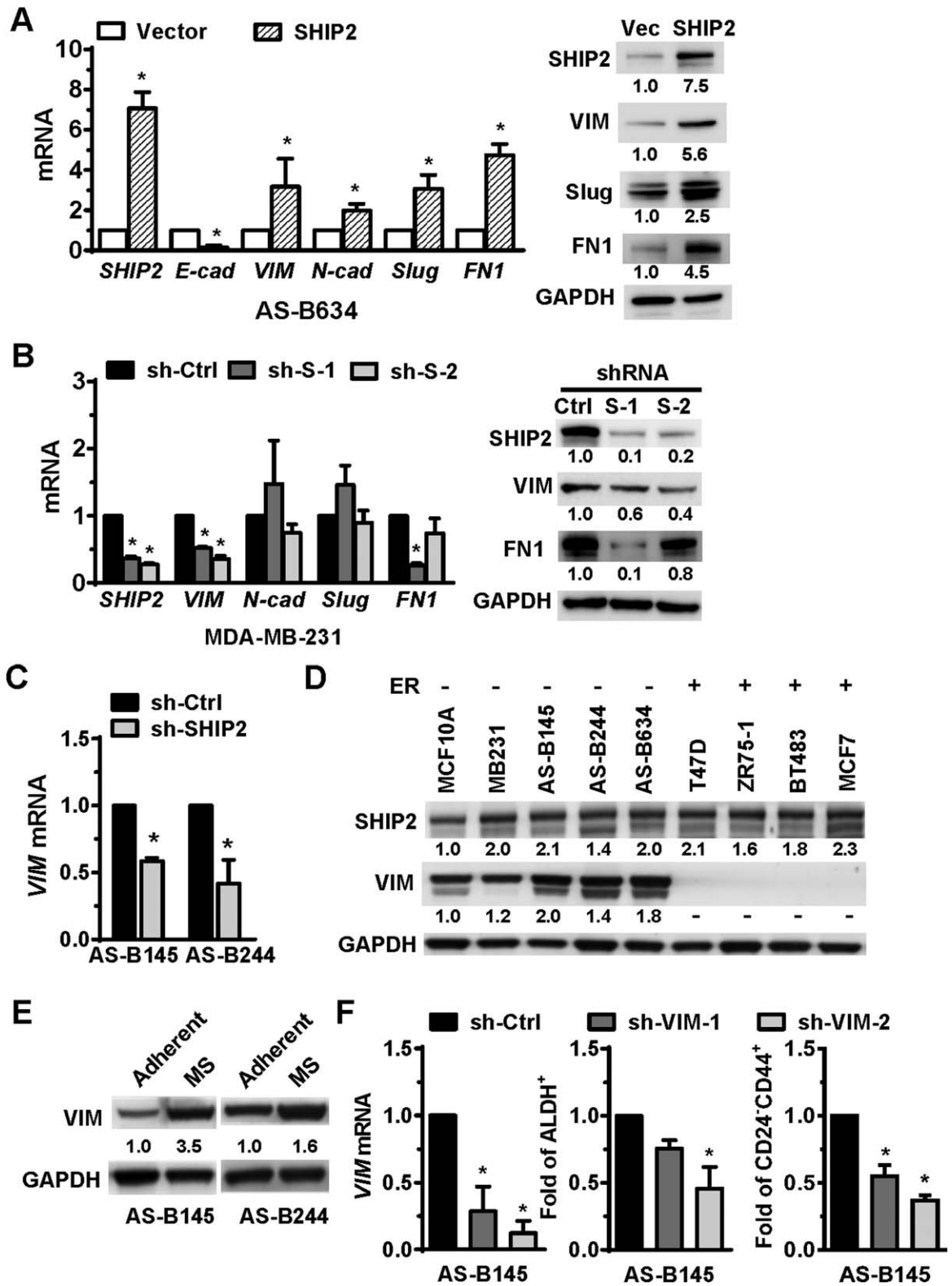

Figure 5. SH2-containing-5′-inositol phosphatase-2 (SHIP2) positively regulates the expression of vimentin (VIM). **(A):** The mRNA and protein expression of EMT-related genes in a SHIP2-overexpressing stable clone and vector control clone of AS-B634 cells was determined by quantitative polymerase chain reaction (qPCR) and Western blots, respectively. **(B):** Four days after SHIP2 knockdown, the mRNA and protein expression of indicated genes in MDA-MB-231 cells was determined by qPCR and Western blots, respectively. **(C):** The expression of *VIM* mRNA in AS-B145 and AS-B244 cells 4 days after SHIP2 knockdown was analyzed by qPCR. **(D):** The expression of SHIP2 and VIM proteins in the indicated cell lines was determined by Western blots. The protein level in each cell line was compared with MCF10A and presented as relative fold. VIM "−": VIM expression was undectable. **(E):** Adherent monolayer cells and mammospheres (MSs) from AS-B145 or AS-B634 cells were harvested to analyze the expression of VIM by Western blots. **(F):** Four days after silencing VIM with the shRNAs in AS-B145 cells, the expression of *VIM* mRNA was analyzed by qPCR and the population of aldehyde dehydrogenase ($ALDH^+$) cells and $CD24^-CD44^+$ was examined by flow cytometry. Data were shown as mean ± SD. *, $p < .05$. Abbreviations: FN1, fibronectin 1; GAPDH, glyceraldehyde 3-phosphate dehydrogenase; SHIP2, SH2-containing-5′-inositol phosphatase-2; shRNA, short hairpin RNA; VIM, vimentin; ER, estrogen receptor.

JNK, a kinase known to phosphorylate c-Jun which drove VIM transcription [32]. We first delineated the role of JNK in BCSCs by comparing the levels of phospho-JNK and JNK proteins in BCSCs and non-BCSCs. As shown in Figure 6A, phospho-p54 JNK was elevated by 2.4- and 2.1-fold in BCSCs sorted from BC0145 ($CD24^-CD44^+$) and BC0244 ($ALDH^+$), as compared to their respective non-BCSCs. The total JNK protein was also higher in BCSCs of both xenografts, especially in BC0244 (up to 9.2-fold for p54 JNK). Moreover, higher phospho-JNK levels (3.3- to 4.4-fold) were observed in mammospheres of AS-B634 cells than adherent monolayer culture, while SP600125, a chemical inhibitor for JNK, suppressed the MFE of AS-B145 cells from $6.2 \pm 0.5\%$ (DMSO) to $5.0 \pm 0.6\%$ at 4 μM and $3.3 \pm 0.6\%$ at 20 μM (Fig. 6B). We further demonstrated that a SHIP2-overexpressing stable clone of AS-B634 cells displayed elevated phospho-JNK expression, especially p54 JNK (fivefold). On the other hand, SHIP2 silencing in AS-B145 cells impaired the activation of p54 and p46 JNK (0.5- and 0.4-fold) (Fig. 6C). We next investigated the interrelationship among JNK, VIM, and SHIP2. As shown in Figure 6D, upon silencing of JNK in AS-B634 cells by shRNAs to 0.04 ± 0.02 (sh-JNK1) and $0.3- \pm 0.03$-fold (sh-JNK2) of sh-Ctrl, the expression of *VIM* mRNAs decreased to $0.5- \pm 0.04$-fold and $0.6- \pm 0.07$-fold, respectively. Similar results were observed in JNK1- or JNK2-silenced SHIP2-overexpressing stable clone of AS-B634 cells with reduced *VIM* mRNA expression to $0.2- \pm 0.1$-fold and $0.1- \pm 0.03$-fold, respectively (Fig. 6E). Moreover, shRNA silencing of JNK1, JNK2 or VIM in SHIP2-overexpressing stable clone of AS-B634 cells dramatically impaired the percentage of $ALDH^+$ population to 0.3 ± 0.004 (sh-JNK1), 0.09 ± 0.03 (sh-JNK2), $0.2- \pm 0.09$-fold (sh-VIM-1), and $0.25- \pm 0.01$-fold (sh-VIM-2) of control cells and reduced the tumorigenicity in vivo with no tumors observed up to 2 months (Fig. 6F). Taken together, these results supported the notion that JNK participated in SHIP2 regulation of VIM expression in ER-negative breast cancers and contributed to the maintenance of the properties of BCSCs. Since VIM has been reported to be phosphorylated by Akt1 in soft-tissue sarcoma cells [33], we investigated the interrelationship between Akt, JNK, and VIM. As shown in Supporting Information Figure S7A, treatment with Akt inhibitor at 10 μM significantly reduced $ALDH^+$ subpopulation in SHIP2-overexpressing AS-B634 cells from $2.83- \pm 0.95$-fold to $0.48- \pm 0.12$-fold increase, as compared to vector control cells. This is consistent with our previous report that Akt activity is essential for the maintenance of features of BCSCs [26], whereas, inhibition of Akt did not attenuate the upregulation of VIM and phospho-JNK levels induced by SHIP2 overexpression in AS-B634 cells (Supporting Information Fig. S7B and C). In summary, SHIP2 is crucial for sustaining the properties of ER-negative BCSCs through its activation of both Akt and JNK with upregulation of VIM.

Discussion

In this report, we assessed the expression of SHIP2 and the percentage of BCSCs in freshly harvested clinical specimens by flow cytometry, and demonstrated the novel functional role of SHIP2 in maintaining the features of BCSCs, including their capacity for mammosphere-formation in vitro and tumorigenicity in vivo and their ability to undergo EMT. Indeed, the importance of SHIP2 in breast cancer was corroborated by our analysis of clinical samples, which revealed significant correlations of greater SHIP2 expression with higher percentage of BCSCs, and of higher SHIP2 expression in BCSCs than non-BCSCs with ER-negative status. While the prognostic significance of SHIP2 in breast cancer was reported by Prasad et al. using immunohistochemistry analysis of paraffin-embedded tumor samples [12], our study is the first to demonstrate a novel oncogenic function of SHIP2 for BCSCs.

The involvement of SHIP2 in EMT was supported by its induction of several EMT markers including N-cadherin, FN1, Slug, and VIM. Although VIM is well known marker for EMT, our present study provided first evidence for its involvement in the maintenance of BCSCs. Several transcription factors have been reported to regulate VIM expression, including Slug, SIP1/ZEB2, Sp1, and c-Jun [32, 34–36]. c-Jun was shown to promote the invasiveness of ErbB2-induced breast cancer and expansion of BCSC through stem cell factor (SCF) and chemokine (C-C motif) ligand 5 (CCL5) [37]. C-Jun is activated by phosphorylation via JNK. The latter is important for the survival of $CD133^+Nestin^+$ glioma stem-like cells [38], but its role in BCSCs has not been delineated. Our results revealed that the levels of phospho-JNK and JNK proteins were higher in BCSCs than non-BCSCs, and JNK inhibitor impaired mammosphere-forming capacity of breast cancer, suggesting its importance in BCSCs. We further demonstrated the activation of JNK by SHIP2 which in turns upregulated VIM expression. Although SHIP2 was reported to activate JNK through interacting with JIP1, we could not detect JIP1 in the SHIP2 immunoprecipitate of AS-B145 and AS-B244 cells (Supporting Information Fig. S8). Thus, the mechanism of SHIP2-induced JNK activation in BCSCs awaits further investigation.

The role of SHIP2 in different cancer types is controversial. It has been reported that overexpression of SHIP2 reduced the growth of erythroleukemia cells [39] and promoted cell cycle arrest in glioblastoma cells [40]. This is in line with SHIP1, a homologue of SHIP2, which was reported to function as a tumor suppressor in leukemia [41, 42]. In contrast, previous reports by Prasad et al. supported the notion that SHIP2 acted as an oncogene in breast cancer through positive regulation of EGFR/Akt pathway [10, 11]. Consistent with this, we also observed regulation of Akt phosphorylation by SHIP2. Several lines of evidence have supported the importance of Akt activation in maintaining CSC characteristics [43–45], including our recent report that insulin-like growth factor-1 receptor (IGF-1R) is critical in maintaining the features of BCSCs through its downstream PI3K/Akt/mTOR pathway [26]. Thus, it is possible that the upstream regulator/regulators of SHIP2-mediated Akt activation may involve EGFR and/or IGF-1R. In this study, we further documented that the oncogenic role of SHIP2 in BCSCs also relied on JNK/VIM activation. Taken together, our findings indicated that SHIP2 might serve as a therapeutic target for eradication of BCSCs through reducing its expression or inositol phosphatase activity. On the other hand, the use of SHIP2 inhibitor for the inositol phosphatase activity has been suggested to be a therapeutic strategy for improving insulin sensitivity in type 2 diabetes mellitus [46–50]. However, the role of SHIP1/2 enzymatic activity for PI3K/Akt activation was contradictory in different types of cells, it might be explained by the "two phosphatidylinositol phosphates (PIP) hypothesis" which suggested that the balance between PI(3,4,5)P3 and PI(3,4)P2 might regulate

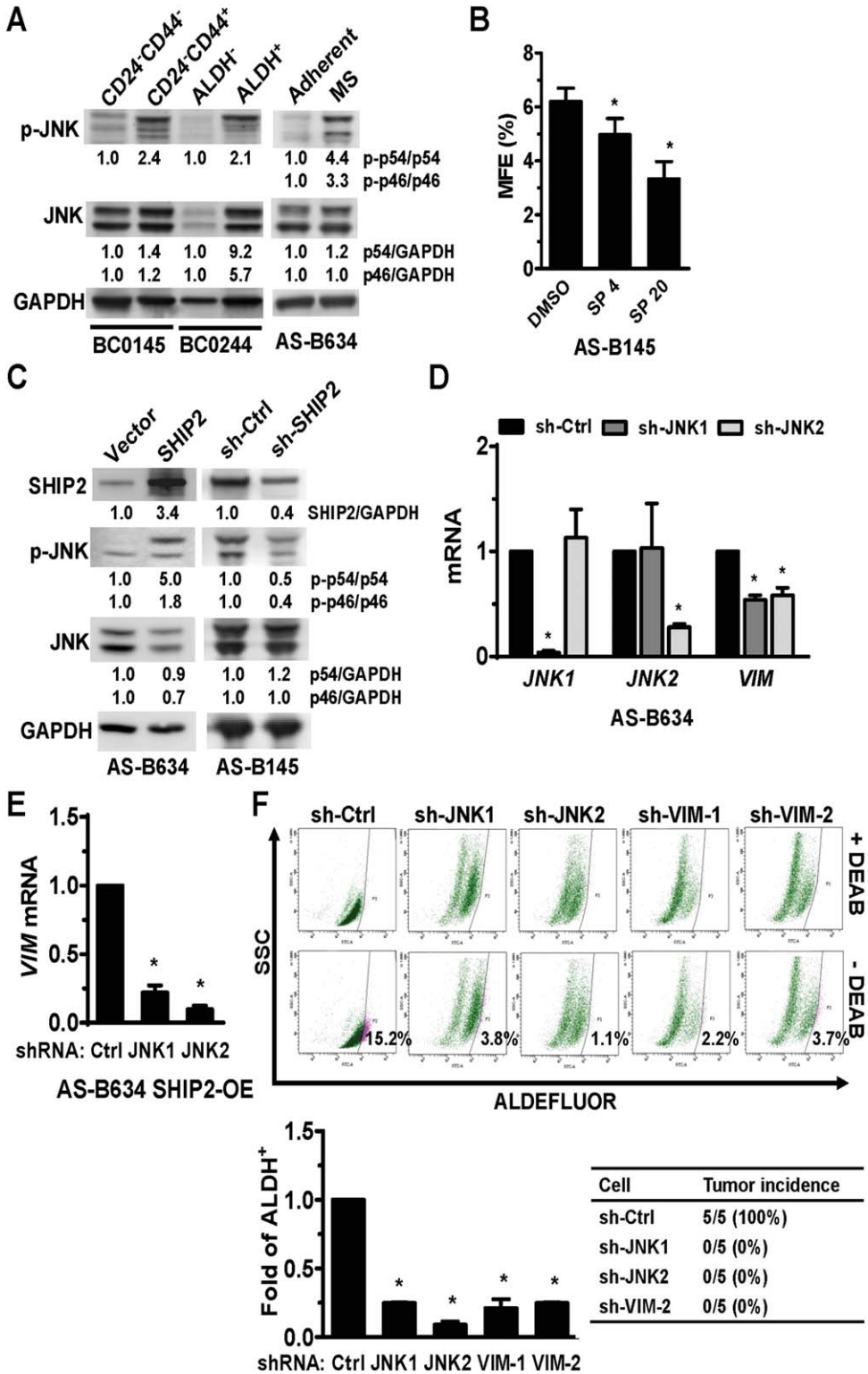

Figure 6. c-Jun *N*-terminal kinase (JNK) participates in the regulation of vimentin by SH2-containing-5′-inositol phosphatase-2 (SHIP2). **(A):** The breast cancer stem cells (BCSCs) (BC0145-CD24$^-$CD44$^+$ and BC0244-ALDH$^+$) and non-BCSCs (BC0145-CD24$^-$CD44$^-$ and BC0244-ALDH$^-$) sorted from xenografts, and adherent monolayer cells or mammosphere (MS) from AS-B634 cells, were collected to determine the amounts of JNK and its phosphoproteins by Western blot. **(B):** After incubation with SP600125 (4 μM, SP4; 20 μM, SP 20) for 2 days, AS-B145 cells were harvested to determine their MS-forming efficiency (MFE). **(C):** The expression of SHIP2, phospho-JNK, and JNK proteins in SHIP2-overexpressing AS-B634 cells or in SHIP2-silenced AS-B145 cells, was determined by Western blot. **(D, E):** JNK1 and JNK2 in AS-B634 cells or SHIP2-overexpressing AS-B634 cells (AS-B634 SHIP2-OE) were knocked down by specific shRNAs for 4 days, and the mRNA level of the indicated genes was determined by qPCR. Data were shown as mean $\pm$ SD from three independent experiments. **(F):** The percentage of aldehyde dehydrogenase (ALDH$^+$) population (upper and lower left panels) in SHIP2-overexpressing stable clone of AS-B634 cells after silencing JNK1, JNK2, or vimentin (VIM), and their tumorigenicity (lower right panel) was evaluated. $n = 5$/group. *, $p < .05$. Fluorescence-activated cell sorting plots were representative of two independent experiments. Abbreviations: DEAB, diethylaminobenzaldehyde; DMSO, dimethyl sulfoxide; GAPDH, glyceraldehyde 3-phosphate dehydrogenase; JNK, c-Jun *N*-terminal kinase 1; SHIP2, SH2-containing-5′-inositol phosphatase-2; MFE, mammosphere-forming efficiency; p-JNK, phospho-JNK; shRNA, short hairpin RNA; VIM, vimentin.

Akt phosphorylation at Thr308 and Ser473, respectively, modulating cell survival [27, 51–56]. While SHIP2 is ubiquitously expressed in hematopoietic lineage and non-hematopoietic tissues including the heart, placenta and skeletal muscles [57, 58], SHIP2 knockout mice survived into adulthood beyond their first year and appeared to grow slowly with resistance to dietary obesity [59]. Hence, it will be worthwhile to develop BCSC-directed therapeutic strategies for some subtypes breast cancers such as ER-negative breast cancers by targeting SHIP2 and its related pathway in the future.

Conclusion

Our study is the first to demonstrate that SHIP2 is crucial for maintaining the properties of BCSCs. This was supported by a positive correlation of the percentage of $SHIP2^+$ cells with that of BCSCs. Within ER-negative breast cancer, there was a significant correlation of greater expression of SHIP2 in BCSCs than non-BCSCs. By gene silencing and overexpression, we documented a novel functional role of SHIP2 in enhancing mammosphere formation and $ALDH^+$ subpopulation in vitro, promoting tumorigenicity in vivo and inducing the expression of EMT markers including VIM. The upregulation of VIM was mediated by JNK activation, which was not mediated by SHIP2-induced Akt activation. Furthermore, the phosphatase activity of SHIP2 also contributed to its role in BCSCs. In summary, our study has uncovered an oncogenic role of SHIP2 in promoting BCSC features and its underlying molecular mechanisms, providing the impetus for the design of novel BCSC-directed therapeutics by targeting SHIP2.

Acknowledgments

We thank Dr. Wen-Hwa Lee for providing ZR75-1, a breast cancer cell line; the National RNAi Core Facility, Academia Sinica, Taipei, Taiwan, for providing lentiviral plasmids; the cell imaging and flow cytometry facilities of the Division of Medical Biology, Genomics Research Center, Academia Sinica, Taipei, Taiwan, for providing excellent service assisted by Li-Wen Lo and Wen-Wen Chen; and nurses Pei-Lan Hsu, Tzu-Yin Yeh, and Hsiang-Min Kung for collecting clinical information of samples; Chun-Wei Hsu, Nai-Chuan Chang, and Hsing-Chieh Ke for providing technical assistance; and Drs. Jung-Tung Hung and Jing-Rong Huang for providing advice and suggestions to this work. This work was supported by Academia Sinica, Chang Gung Medical Foundation and National Science Council grants (NSC97-2323-B-001 and NSC 100-2321-B-001-037 [to A.L.Y.]; NSC100-2321-B-001-036 and NSC101-2321-B-001-023 [to J.Y.]; NSC-100-2314-B-040-013 [to W.W.C.]).

Author Contributions

C.-H.F.: conception and design, collection and/or assembly of data, data analysis and interpretation, manuscript writing, and final approval of manuscript; R.-J.L.: collection and/or assembly of data, and data analysis and interpretation, and manuscript revision; J.Y.: financial support, manuscript writing, and final approval of manuscript; W.-W.C. and W.-Y.C.: collection of data; G.-S.L., L.-M.T., and Y.-F.T.: provision of study material and patients; J.-C.Y.: provision of study material and patients, data interpretation and manuscript revision; A.L.Y.: conception and design, financial support, data analysis and interpretation, manuscript writing, and final approval of manuscript.

Disclosure of Potential Conflicts of Interest

The authors indicate no potential conflicts of interest.

References

1 Lapidot T, Sirard C, Vormoor J, et al. A cell initiating human acute myeloid leukaemia after transplantation into SCID mice. Nature 1994;367:645–648.

2 Singh SK, Clarke ID, Terasaki M, et al. Identification of a cancer stem cell in human brain tumors. Cancer Res 2003;63:5821–5828.

3 Ricci-Vitiani L, Lombardi DG, Pilozzi E, et al. Identification and expansion of human colon-cancer-initiating cells. Nature 2007;445:111–115.

4 Al-Hajj M, Wicha MS, Benito-Hernandez A, et al. Prospective identification of tumorigenic breast cancer cells. Proc Natl Acad Sci U S A 2003;100:3983–3988.

5 Li C, Heidt DG, Dalerba P, Burant CF, et al. Identification of pancreatic cancer stem cells. Cancer Res 2007;67:1030–1037.

6 Ginestier C, Hur MH, Charafe-Jauffret E, et al. ALDH1 is a marker of normal and malignant human mammary stem cells and a predictor of poor clinical outcome. Cell Stem Cell 2007;1:555–567.

7 Hermann PC, Huber SL, Herrler T, et al. Distinct populations of cancer stem cells determine tumor growth and metastatic activity in human pancreatic cancer. Cell Stem Cell 2007;1:313–323.

8 Dean M, Fojo T, Bates S. Tumour stem cells and drug resistance. Nat Rev Cancer 2005;5:275–284.

9 Rich JN. Cancer stem cells in radiation resistance. Cancer Res 2007;67:8980–8984.

10 Prasad NK, Tandon M, Badve S, et al. Phosphoinositol phosphatase SHIP2 promotes cancer development and metastasis coupled with alterations in EGF receptor turnover. Carcinogenesis 2008;29:25–34.

11 Prasad NK. SHIP2 phosphoinositol phosphatase positively regulates EGFR-Akt pathway, CXCR4 expression, and cell migration in MDA-MB-231 breast cancer cells. Int J Oncol 2009;34:97–105.

12 Prasad NK, Tandon M, Handa A, et al. High expression of obesity-linked phosphatase SHIP2 in invasive breast cancer correlates with reduced disease-free survival. Tumour Biol 2008;29:330–341.

13 Clement S, Krause U, Desmedt F, et al. The lipid phosphatase SHIP2 controls insulin sensitivity. Nature 2001;409:92–97.

14 Ishihara H, Sasaoka T, Hori H, et al. Molecular cloning of rat SH2-containing inositol phosphatase 2 (SHIP2) and its role in the regulation of insulin signaling. Biochem Biophys Res Commun 1999;260:265–272.

15 Fuhler GM, Brooks R, Toms B, et al. Therapeutic potential of SH2 domain-containing inositol-5′-phosphatase 1 (SHIP1) and SHIP2 inhibition in cancer. Mol Med 2012;18:65–75.

16 Vandenbroere I, Paternotte N, Dumont JE, et al. The c-Cbl-associated protein and c-Cbl are two new partners of the SH2-containing inositol polyphosphate 5-phosphatase SHIP2. Biochem Biophys Res Commun 2003;300:494–500.

17 Prasad NK, Decker SJ. SH2-containing 5′-inositol phosphatase, SHIP2, regulates cytoskeleton organization and ligand-dependent down-regulation of the epidermal growth factor receptor. J Biol Chem 2005;280:13129–13136.

18 Prasad N, Topping RS, Decker SJ. SH2-containing inositol 5′-phosphatase SHIP2 associates with the p130(Cas) adapter protein and regulates cellular adhesion and spreading. Mol Cell Biol 2001;21:1416–1428.

19 Dyson JM, O'Malley CJ, Becanovic J, et al. The SH2-containing inositol polyphosphate 5-phosphatase, SHIP-2, binds filamin and regulates submembraneous actin. J Cell Biol 2001;155:1065–1079.

20 Paternotte N, Zhang J, Vandenbroere I, et al. SHIP2 interaction with the cytoskeletal protein Vinexin. FEBS J 2005;272:6052–6066.

21 Koch A, Mancini A, El Bounkari O, et al. The SH2-domian-containing inositol 5-phosphatase (SHIP)-2 binds to c-Met directly via tyrosine residue 1356 and involves hepatocyte growth factor (HGF)-induced lamellipodium formation, cell scattering and cell spreading. Oncogene 2005;24:3436–3447.
22 Zhuang G, Hunter S, Hwang Y, et al. Regulation of EphA2 receptor endocytosis by SHIP2 lipid phosphatase via phosphatidylinositol 3-Kinase-dependent Rac1 activation. J Biol Chem 2007;282:2683–2694.
23 Leone M, Cellitti J, Pellecchia M. NMR studies of a heterotypic Sam-Sam domain association: The interaction between the lipid phosphatase Ship2 and the EphA2 receptor. Biochemistry 2008;47:12721–12728.
24 Xie J, Onnockx S, Vandenbroere I, et al. The docking properties of SHIP2 influence both JIP1 tyrosine phosphorylation and JNK activity. Cell Signal 2008;20:1432–1441.
25 Chang WW, Lee CH, Lee P, et al. Expression of Globo H and SSEA3 in breast cancer stem cells and the involvement of fucosyl transferases 1 and 2 in Globo H synthesis. Proc Natl Acad Sci U S A 2008;105:11667–11672.
26 Chang WW, Lin RJ, Yu J, et al. The expression and significance of insulin-like growth factor-1 receptor and its pathway on breast cancer stem/progenitors. Breast Cancer Res 2013;15:R39.
27 Suwa A, Kurama T, Yamamoto T, et al. Glucose metabolism activation by SHIP2 inhibitors via up-regulation of GLUT1 gene in L6 myotubes. Eur J Pharmacol 2010;642:177–182.
28 Shaw FL, Harrison H, Spence K, et al. A detailed mammosphere assay protocol for the quantification of breast stem cell activity. J Mammary Gland Biol Neoplasia 2012;17:111–117.
29 Hu Y, Smyth GK. ELDA: Extreme limiting dilution analysis for comparing depleted and enriched populations in stem cell and other assays. J Immunol Methods 2009;347:70–78.
30 van de Vijver MJ, He YD, van't Veer LJ, et al. A gene-expression signature as a predictor of survival in breast cancer. N Engl J Med 2002;347:1999–2009.
31 Ricardo S, Vieira AF, Gerhard R, et al. Breast cancer stem cell markers CD44, CD24 and ALDH1: Expression distribution within intrinsic molecular subtype. J Clin Pathol 2011;64:937–946.
32 Wu Y, Zhang X, Zehner ZE. c-Jun and the dominant-negative mutant, TAM67, induce vimentin gene expression by interacting with the activator Sp1. Oncogene 2003;22:8891–8901.
33 Zhu QS, Rosenblatt K, Huang KL, et al. Vimentin is a novel AKT1 target mediating motility and invasion. Oncogene 2011;30:457–470.
34 Sommers CL, Skerker JM, Chrysogelos SA, et al. Regulation of vimentin gene transcription in human breast cancer cell lines. Cell Growth Differ 1994;5:839–846.
35 Bindels S, Mestdagt M, Vandewalle C, et al. Regulation of vimentin by SIP1 in human epithelial breast tumor cells. Oncogene 2006;25:4975–4985.
36 Vuoriluoto K, Haugen H, Kiviluoto S, et al. Vimentin regulates EMT induction by Slug and oncogenic H-Ras and migration by governing Axl expression in breast cancer. Oncogene 2011;30:1436–1448.
37 Jiao X, Katiyar S, Willmarth NE, et al. c-Jun induces mammary epithelial cellular invasion and breast cancer stem cell expansion. J Biol Chem 2010;285:8218–8226.
38 Yoon CH, Kim MJ, Kim RK, et al. c-Jun N-terminal kinase has a pivotal role in the maintenance of self-renewal and tumorigenicity in glioma stem-like cells. Oncogene 2012;31:4655–4666.
39 Giuriato S, Blero D, Robaye B, et al. SHIP2 overexpression strongly reduces the proliferation rate of K562 erythroleukemia cell line. Biochem Biophys Res Commun 2002;296:106–110.
40 Taylor V, Wong M, Brandts C, et al. 5′ phospholipid phosphatase SHIP-2 causes protein kinase B inactivation and cell cycle arrest in glioblastoma cells. Mol Cell Biol 2000;20:6860–6871.
41 Gilby DC, Goodeve AC, Winship PR, et al. Gene structure, expression profiling and mutation analysis of the tumour suppressor SHIP1 in Caucasian acute myeloid leukaemia. Leukemia 2007;21:2390–2393.
42 Lo TC, Barnhill LM, Kim Y, et al. Inactivation of SHIP1 in T-cell acute lymphoblastic leukemia due to mutation and extensive alternative splicing. Leuk Res 2009;33:1562–1566.
43 Dubrovska A, Kim S, Salamone RJ, et al. The role of PTEN/Akt/PI3K signaling in the maintenance and viability of prostate cancer stem-like cell populations. Proc Natl Acad Sci U S A 2009;106:268–273.
44 Eyler CE, Foo WC, LaFiura KM, McLendon RE, Hjelmeland AB, Rich JN et al. Brain cancer stem cells display preferential sensitivity to Akt inhibition. Stem Cells 2008;26:3027–3036.
45 Ma S, Lee TK, Zheng BJ, et al. CD133+ HCC cancer stem cells confer chemoresistance by preferential expression of the Akt/PKB survival pathway. Oncogene 2008;27:1749–1758.
46 Sasaoka T, Wada T, Tsuneki H. Lipid phosphatases as a possible therapeutic target in cases of type 2 diabetes and obesity. Pharmacol Ther 2006;112:799–809.
47 Lazar DF, Saltiel AR. Lipid phosphatases as drug discovery targets for type 2 diabetes. Nat Rev Drug Discov 2006;5:333–342.
48 Baumgartener JW. SHIP2: An emerging target for the treatment of type 2 diabetes mellitus. Curr Drug Targets Immune Endocr Metabol Disord 2003;3:291–298.
49 Suwa A, Yamamoto T, Sawada A, et al. Discovery and functional characterization of a novel small molecule inhibitor of the intracellular phosphatase, SHIP2. Br J Pharmacol 2009;158:879–887.
50 Annis DA, Cheng CC, Chuang CC, et al. Inhibitors of the lipid phosphatase SHIP2 discovered by high-throughput affinity selection-mass spectrometry screening of combinatorial libraries. Comb Chem High Throughput Screen 2009;12:760–771.
51 Ma K, Cheung SM, Marshall AJ, et al. PI(3,4,5)P3 and PI(3,4)P2 levels correlate with PKB/akt phosphorylation at Thr308 and Ser473, respectively; PI(3,4)P2 levels determine PKB activity. Cell Signal 2008;20:684–694.
52 Choi Y, Zhang J, Murga C, et al. PTEN, but not SHIP and SHIP2, suppresses the PI3K/Akt pathway and induces growth inhibition and apoptosis of myeloma cells. Oncogene 2002;21:5289–5300.
53 Carver DJ, Aman MJ, Ravichandran KS. SHIP inhibits Akt activation in B cells through regulation of Akt membrane localization. Blood 2000;96:1449–1456.
54 Liu Q, Sasaki T, Kozieradzki I, et al. SHIP is a negative regulator of growth factor receptor-mediated PKB/Akt activation and myeloid cell survival. Genes Dev 1999;13:786–791.
55 Aman MJ, Lamkin TD, Okada H, et al. The inositol phosphatase SHIP inhibits Akt/PKB activation in B cells. J Biol Chem 1998;273:33922–33928.
56 Horn S, Endl E, Fehse B, et al. Restoration of SHIP activity in a human leukemia cell line downregulates constitutively activated phosphatidylinositol 3-kinase/Akt/GSK-3beta signaling and leads to an increased transit time through the G1 phase of the cell cycle. Leukemia 2004;18:1839–1849.
57 Pesesse X, Deleu S, De Smedt F, et al. Identification of a second SH2-domain-containing protein closely related to the phosphatidylinositol polyphosphate 5-phosphatase SHIP. Biochem Biophys Res Commun 1997;239:697–700.
58 Muraille E, Pesesse X, Kuntz C, et al. Distribution of the src-homology-2-domain-containing inositol 5-phosphatase SHIP-2 in both non-haemopoietic and haemopoietic cells and possible involvement of SHIP-2 in negative signalling of B-cells. Biochem J 1999;342 Pt 3:697–705.
59 Sleeman MW, Wortley KE, Lai KM, et al. Absence of the lipid phosphatase SHIP2 confers resistance to dietary obesity. Nat Med 2005;11:199–205.


See www.StemCells.com for supporting information available online.